

FALCON: False-Negative Aware Learning of Contrastive Negatives in Vision-Language Pretraining

Myunsoo Kim* Seong-Woong Shim* Byung-Jun Lee†

Korea University, Decision Making Lab

{m970326, ssw030830, byungjunlee}@korea.ac.kr

Abstract

False negatives pose a critical challenge in vision-language pretraining (VLP) due to the many-to-many correspondence between images and texts in large-scale datasets. These false negatives introduce conflicting supervision signals that degrade the learned embedding space and diminish the effectiveness of hard negative sampling. In this paper, we propose FALCON (False-negative Aware Learning of COntrastive Negatives), a learning-based mini-batch construction strategy that adaptively balances the trade-off between hard and false negatives during VLP. Rather than relying on fixed heuristics, FALCON employs a negative mining scheduler that dynamically selects negative samples of appropriate hardness for each anchor instance during mini-batch construction, guided by a proxy for cross-modal alignment improvement. Experimental results demonstrate that FALCON significantly improves performance across two widely adopted VLP frameworks (ALBEF, BLIP-2) and a broad range of downstream tasks and evaluation settings, underscoring its effectiveness and robustness in mitigating the impact of false negatives.

1 Introduction

The goal of Vision-and-Language Pre-training (VLP) is to learn cross-modal representations from large-scale image-text pairs, improving performance on downstream tasks such as image-text retrieval (IRTR) [1], visual question answering (VQA) [2], and natural language for visual reasoning (NLVR) [3]. Recent advancements [4, 5, 6] have demonstrated remarkable progress in this domain, underscoring the effectiveness of VLP in cross-modal representation learning.

These models are typically trained with self-supervised objectives such as masked language modeling (MLM), image-text contrastive (ITC), and image-text matching (ITM) losses. While ITC and ITM are effective in improving the quality of the learned embedding space, they inherently require negative samples during training. In particular, the inclusion of *hard negatives*—those that are semantically similar to the anchor sample—has been shown to be crucial for the success of VLP [7]. As a result, substantial research efforts have been devoted to devising more effective strategies for choosing such hard negatives [4, 5, 6, 8].

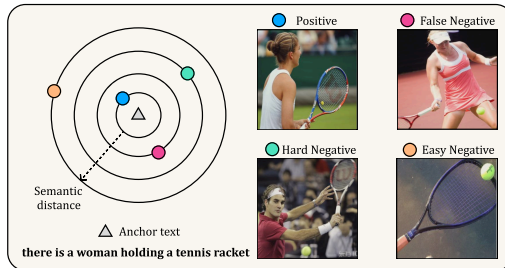


Figure 1: Illustration of semantic distance between an anchor text and multiple image samples in the vision-language embedding space.

*Equal contribution.

†Corresponding author.

Although effective, these hard negative sampling strategies exhibit a critical limitation: as the selection criterion favors negatives with higher semantic similarity to the anchor, the likelihood of mistakenly identifying true positives as negatives (i.e., *false negatives*) correspondingly increases [9] (see Figure 1). This challenge is particularly acute in VLP, where large-scale web-crawled datasets often exhibit many-to-many correspondences between images and text [9, 10]. Incorporating such false negatives into contrastive learning can substantially degrade representation quality by compelling the model to separate embeddings that should ideally remain close within the shared embedding space.

To address this challenge, a few recent works attempted to mitigate this issue by leveraging strong pretrained models, either by refining the loss function to reduce the impact of false negative [10, 11] or relabeling false negatives as positives [9, 12]. However, these methods heavily depend on the reliability of the pretrained models and the heuristics used to identify false negatives, potentially limiting their generalizability across diverse datasets and training settings.

In this paper, we present FALCON (False-negative Aware Learning of COntrastive Negatives), a learning-based mini-batch construction strategy for VLP that adaptively balances the trade-off between informative (hard) negatives and misleading (false) negatives. By explicitly optimizing this trade-off during mini-batch construction, FALCON effectively accounts for the inevitable presence of false negatives, improving the quality of learned cross-modal representations. Our empirical results demonstrate that FALCON significantly outperforms heuristic baselines across a wide range of downstream tasks and evaluation settings.

Due to space constraints, the **detailed discussion on related works** is provided in the Appendix A.

2 Motivation

In this section, we demonstrate that the false negative problem is an inherent and unavoidable challenge in VLP. We further motivate the need for a scheduling strategy that dynamically balances the trade-off between hard and false negatives throughout the VLP process.

Inevitability of false negatives in VLP Given an image-text pair, the text may align with several plausible visual representations, and the image may correspond to multiple semantically valid textual descriptions. This intrinsic many-to-many alignment between visual and textual modalities leads to the unavoidable presence of false negatives in VLP.

Proposition 1. *Let $\mathcal{V} = \{v_1, \dots, v_{|\mathcal{V}|}\}$ denote the set of images and $\mathcal{T} = \{t_1, \dots, t_{|\mathcal{T}|}\}$ the set of texts. Define $\mathcal{R} \subseteq \mathcal{V} \times \mathcal{T}$ as the binary relation of semantic compatibility within the Cartesian product of image and text set, where $(v, t) \in \mathcal{R}$ implies that t is a valid description of v . Let $\mathcal{P} \subset \mathcal{R}$ denote the set of ground-truth positive pairs available to the learner, such that any pair $(v, t) \notin \mathcal{P}$ is treated as negative during vision-language pretraining (VLP). Then, the probability of sampling a false negative remains **strictly positive** unless $\mathcal{P} = \mathcal{R}$, an assumption that is infeasible in practice.*

The proof is provided in the Appendix B. Note that the theoretical corner case $\mathcal{P} = \mathcal{R}$, which corresponds to a setting where all semantically compatible image-text pairs are known and labeled as positives, is infeasible in practice as soon as we account for the presence of synonyms, paraphrases, and stylistic or distributional variations introduced by human or AI-generated annotations [13, 14, 15, 16]. These factors render the space of valid image-text alignments effectively infinite, making the complete manual identification and exclusion of false negatives impractical.

Optimal similarity is anchor-specific and evolves over training To retrieve hard negatives, prior works have commonly adopted cosine similarity of embeddings as a selection criterion [4, 5, 6, 8, 9], selecting images or texts with high similarity to the anchor. It is widely acknowledged that there exists an optimal similarity range that facilitates effective hard negative mining while minimizing the risk of false negative inclusion [17, 18]. However, this optimal range is inherently anchor-specific and evolves throughout the training process, making it impractical to capture with a single fixed similarity level. In particular, semantically complex anchors are more difficult to align and are therefore learned more slowly, resulting in less mature and noisier embeddings even in later stages of training. For such anchors, or during the early phases of training, selection of negatives with sufficiently low similarity is necessary to reduce the risk of false negatives. In contrast, semantically simple anchors are aligned more rapidly and yield well-formed embeddings earlier in training. In these cases, or in the later stage

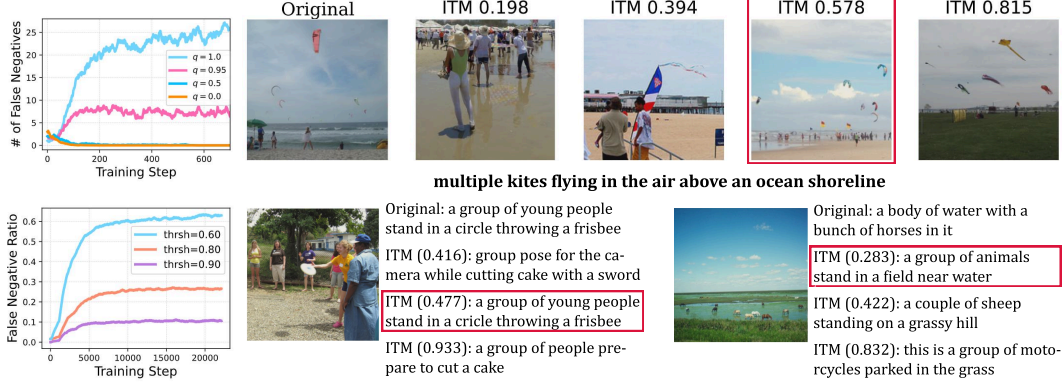


Figure 2: **(Top Left)** Risk of false negatives across training steps for different similarity quantiles q used in mini-batch construction during VLP [8]. False negatives are identified using the pretrained BLIP-129M model [5]. **(Bottom Left)** False negative ratio during VLP when false negative filtering is applied using the pretrained model’s ITM score at varying thresholds. On the right, Text-to-Image **(Top Right)** and Image-to-Text **(Bottom Right)** examples are shown where the pretrained model fails to assign high ITM scores to false negatives. Instances highlighted in red represent false negatives.

of training, the similarity distribution of positive pairs becomes tighter and concentrated at higher values, permitting the safe mining of more similar negatives.

Consequently, VLP methods that rely on embedding similarity are exposed to a dynamic, anchor-dependent risk of false negative selection that evolves throughout the training process. As shown in Figure 2 (top left), the false negative rate increases substantially when highly similar samples ($q = 1.0$) are selected for mini-batch construction during vision-language pretraining. Here, $q \in [0, 1]$ denotes the quantile level used to define the hardness of negative samples within the candidate pool. Over the course of training, false negatives associated with simple semantic anchors progressively cluster in the upper quantiles of the similarity spectrum, exacerbating the risk associated with high- q negative sampling (i.e., aggressive hard negative sampling). Conversely, selecting less similar samples ($q \leq 0.5$) results in a progressively lower incidence of false negatives throughout training. These findings emphasize the need for an adaptive strategy that dynamically adjusts the similarity threshold based on the anchor’s semantic characteristics and the evolving state of the embedding space.

Adoption of pretrained models is not a complete solution To address this challenge, prior works have leveraged strong pretrained models (e.g., BLIP with 129M parameters) to detect potential false negatives in image-text pairs [10, 11, 9, 12]. For example, MAFA [9] uses the Image-Text Matching (ITM) score predicted by a pretrained model to identify false negatives, relabeling them as positives when the score exceeds a predefined threshold. While this approach mitigates the nonstationarity associated with learned similarity metrics—since the pretrained model remains fixed throughout training—its effectiveness is still limited by the anchor-specific nature of the scores. For simple descriptions or images, the set of valid positive samples is typically large and diverse, enabling pretrained models to easily assign high ITM scores to positives (and false negatives). In contrast, pretrained models struggle to generalize in more complex scenarios due to limited prior exposure, often assigning low ITM scores even to semantically aligned pairs (see Figure 2, right). Consequently, applying a fixed ITM threshold would be either overly conservative for simple pairs or insufficient to eliminate false negatives in complex pairs.

Furthermore, the conventional two-stage framework, which selects the most similar negatives followed by filtering with a pretrained model [9], is highly sensitive to hyperparameter choices, since the initial stage often includes a substantial proportion of false negatives. If the filtering threshold of the pretrained model is misspecified, training can be severely hindered by an excessively high false negative rate, reaching up to 60% (see Figure 2, bottom left).

3 Main Method

Recent VLP models [4, 5, 6] are typically optimized using a combination of contrastive and generative objectives, as expressed by the following loss formulation:

$$\min_{\theta} \mathcal{L}_{\text{VLP}}(\theta) := \mathbb{E}_{(V,T) \sim \mathcal{V}, \mathcal{T}} [\mathcal{L}_{\text{ITC}}(V, T; \theta) + \mathcal{L}_{\text{ITM}}(V, T; \theta) + \mathcal{L}_{\text{MLM}}(V, T; \theta)]. \quad (1)$$

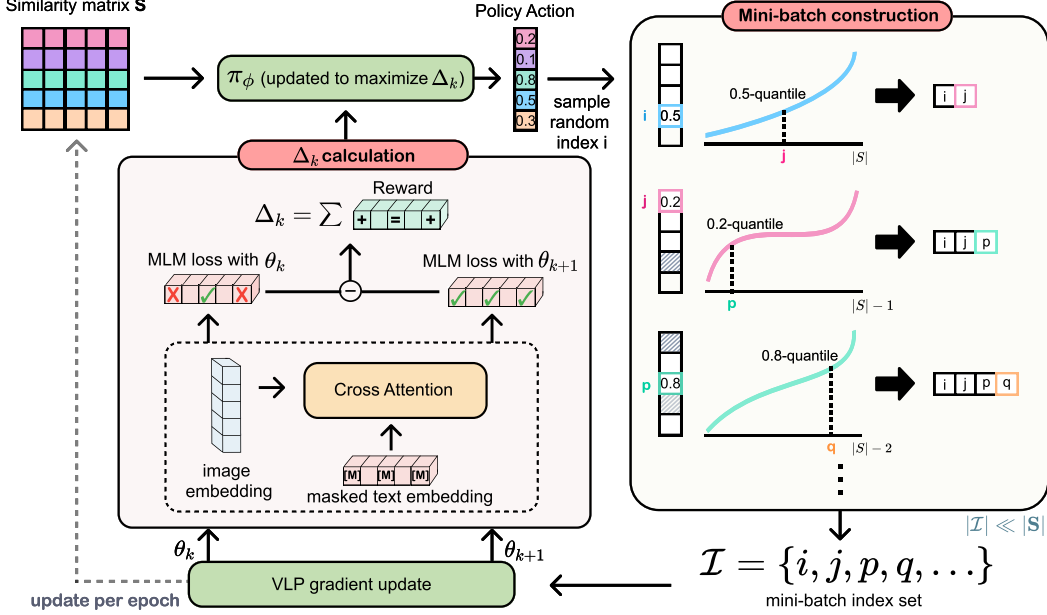


Figure 3: Overview of FALCON, a learning-based mini-batch construction strategy for VLP. Starting from a randomly selected anchor, the scheduler π_ϕ predicts hardness quantile values to iteratively sample additional candidates, forming a mini-batch index set \mathcal{I} . This batch is used to update the VLP model. The reduction in masked language modeling loss \mathcal{L}_{MLM} serves as a proxy for enhanced cross-modal alignment, providing a reward signal that guides the scheduler toward constructing more informative mini-batches in subsequent training steps.

where θ denotes the parameters of the VLP model, \mathcal{L}_{ITC} , \mathcal{L}_{ITM} , and \mathcal{L}_{MLM} correspond to the image-text contrastive (ITC) loss, image-text matching (ITM) loss, and masked language modeling (MLM) loss, respectively. In particular, ITC serves as a contrastive loss that aligns embeddings for matched image-text pairs (positive pair) while pushing apart mismatched pairs (negative pair) in the embedding space. Complementarily, ITM is a binary matching objective that further distinguishes positive and negative pairs, enhancing cross-modal alignment. The MLM loss can be replaced with alternative generative objectives, e.g., the BLIP family [5, 6].

Due to the inclusion of contrastive objectives (ITC, ITM), the quality of the learned embedding space is strongly influenced by the hardness of the negative samples [7, 4, 5]. Traditionally, each instance within a mini-batch serves as an anchor, with all remaining instances in the same batch acting as its negative samples. As such, the composition of the mini-batch critically influences both the quality and the difficulty of the negative samples [19, 4, 8]. However, as discussed in the previous section, existing strategies for mini-batch construction have not sufficiently accounted for the anchor-dependent and training-dependent variability in optimal negative sample hardness.

In this section, we present FALCON, a learning-based mini-batch construction strategy that adaptively balances hard and false negatives by optimizing a scheduler π_ϕ to determine an appropriate negative hardness level for each anchor during mini-batch construction in VLP

3.1 Construction of Mini-batch using Negative Mining Scheduler

While the VLP loss (1) was initially proposed with conventional uniform sampling of a mini-batch (V, T) , GRIT-VLP [8] modifies the sampling procedure by introducing a mini-batch grouping strategy that iteratively selects the sample most semantically similar to the most recently chosen sample, thereby promoting more effective hard negative mining within each batch. For scalability, the dataset is partitioned into multiple localized search spaces $\{M\}$ and the most similar sample is searched within the search space. However, GRIT-VLP does not account for the heightened risk of false negatives associated with mining increasingly harder negatives, which substantially limits the effectiveness of hard negative sampling; for example, excessively large search space size $|M|$ can lead to performance degradation due to the elevated likelihood of false negatives (see Appendix D.3).

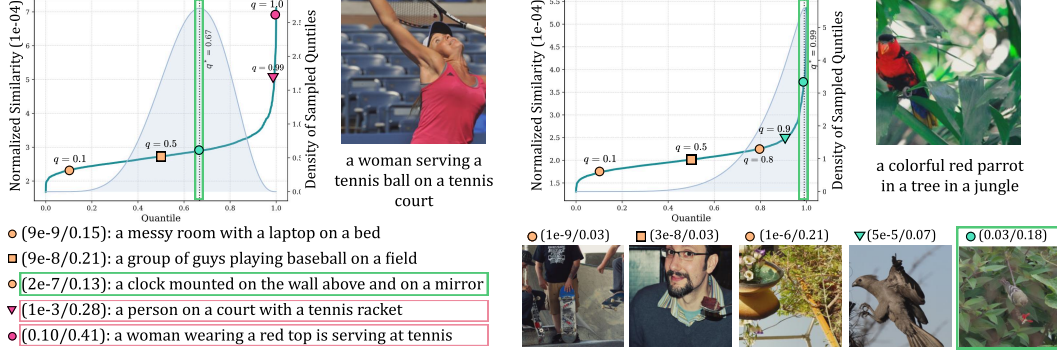


Figure 4: Image-to-Text (Left) and Text-to-Image (Right) examples illustrating FALCON’s quantile-based negative sampling strategy. For each anchor query (shown adjacent to each plot), the normalized similarity distribution \hat{S} over the candidate set is displayed alongside the scheduler’s predicted distribution on quantiles (blue-shaded density curve). Sampled negatives are annotated with their (one-way similarity / pretrained ITM score), and color-coded by hardness level as defined in Figure 1.

To this end, we extend the strategy of GRIT-VLP by selecting the next sample based on a specified level of similarity to the most recently chosen sample, where the similarity level is determined by a scheduler π_ϕ rather than fixed to the most similar sample. By jointly optimizing the scheduler during training, we aim to adaptively balance the trade-off between hard and false negatives by dynamically selecting the appropriate similarity level on a per-instance basis during mini-batch construction.

Specifically, the scheduler π_ϕ predicts a hardness quantile value $q \in [0, 1]$ for each anchor. When the scheduler determines that an anchor would benefit from more informative and challenging negatives under the current state of the VLP model, it samples a quantile value closer to 1, thereby selecting harder negatives. Note that a scheduler consistently producing $q = 1$ effectively reduces to the GRIT-VLP strategy. Conversely, when the potential risk of sampling false negatives is high, the scheduler assigns a lower quantile value, favoring negatives that are semantically dissimilar and thus less likely to overlap with true positives.

A detailed mini-batch construction process is illustrated in Figure 3, with corresponding pseudo-code provided in Appendix C.1. The process begins by uniformly selecting an initial sample from the local search space. Then, a new sample is chosen according to the hardness quantile value q predicted by the scheduler π_ϕ , and added to the mini-batch. This procedure is applied recursively until a mini-batch of size B is formed: at each step, a new sample is selected using the hardness quantile, excluding previously selected samples from further selection. Once the mini-batch is constructed, it is used to update the VLP model parameterized by θ . As the size of search space M is larger than the mini-batch size B , the procedure of constructing mini-batches and updating the VLP model is repeated iteratively until all candidates within the search space have been utilized. Through this tactical grouping strategy, negative samples that align with the desired hardness level for each anchor are progressively incorporated into the VLP process (more details in Appendix C.2).

3.2 Design of Negative Mining Scheduler

To enable the scheduler π_ϕ to adaptively select negative samples with appropriate hardness for each anchor instance during mini-batch construction, we provide it with a matrix of similarity distributions computed over samples within the search space. Instead of feeding the anchor instances directly into the scheduler, we use the distribution of similarities between the anchor and the candidate samples, represented by the corresponding rows of the similarity distribution matrix. This serves as an efficient surrogate for estimating the similarity levels required to identify suitable hard negatives.

Specifically, we construct a unified similarity matrix S by adding the image-to-text (I2T) and text-to-image (T2I) pairwise similarity matrices among candidates within the local search space. These matrices are computed from the [CLS] embeddings of image and text representations and contain rich information about the semantic alignment between modalities in the representation space. Following prior works, we leverage cached [CLS] embeddings maintained in a queue to compute S , thereby avoiding additional forward passes [19, 4, 8].

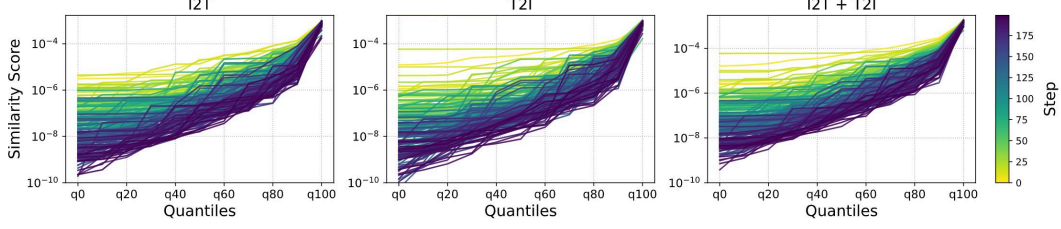


Figure 5: Visualization of normalized cosine similarity distributions across training during VLP. Each plot shows the similarity scores at different quantile levels for I2T (left), T2I (center), and I2T+T2I (right), with the color bar indicating training progression. Step values are shown in thousands (K).

By integrating both I2T and T2I similarities into a single matrix, the scheduler π_ϕ can operate in a direction-agnostic manner, thereby eliminating the need to alternate between modalities during negative sample selection. Figure 5 visualizes similarity distributions of both I2T and T2I; as the two matrices exhibit comparable scales, we did not employ a more complex combination strategy.

To facilitate efficient learning of similarity distributions, we select m evenly spaced quantiles from each row instead of using the full set of raw similarity values, yielding a compact matrix of size $|M| \times m$ where $m \ll |M|$. Afterwards, row-wise normalization using softmax is applied to minimize the impact of changing scale of pairwise similarities over training (see Figure 5). We call this normalized similarity distribution matrix $\hat{\mathbf{S}}$.

The scheduler π_ϕ is implemented as a lightweight 4-layer residual MLP that maps $\hat{\mathbf{S}}$ to the parameters (α, β) of Beta distributions, which model the desired hardness (similarity quantile) of negative samples for each anchor. To ensure permutation equivariance over rows without relying on heavier architectures [20, 21, 22], we sort the rows of $\hat{\mathbf{S}}$ prior to inputting it into the MLP [23]. This design choice offers great computational and memory efficiency while maintaining sufficient expressivity for the scheduling task. Figure 4 presents qualitative examples of FALCON’s quantile-based sampling.

3.3 Training Negative Mining Scheduler

The goal of VLP is to learn a unified representation space that effectively aligns visual and textual modalities, thereby enabling generalization across a wide range of downstream multimodal tasks. To support this objective, we design the training signal for π_ϕ to encourage mini-batch constructions that enhance cross-modal alignment within the learned representation space.

Specifically, we formulate the objective as **maximizing the reduction in the masked language modeling loss** \mathcal{L}_{MLM} measured before and after updating the VLP model with a mini-batch constructed by π_ϕ , while keeping the masking identical for loss evaluations.³ This change in \mathcal{L}_{MLM} serves as a proxy for improvements in the model’s ability to integrate visual context into language understanding via cross-attention, thus reflecting more refined semantic alignment between the two modalities. In contrast, training π_ϕ to minimize other objectives (e.g., \mathcal{L}_{ITC} , \mathcal{L}_{ITM}) that rely on negative samples undermines VLP training by encouraging the exploitation of trivial negatives, which is empirically validated in our experiments.

Formally, we aim to update our scheduler π_{ϕ_k} at the k -th gradient update step as:

$$\phi_k = \arg \max_{\phi_k} \mathbb{E}_{(V,T) \sim \pi_{\phi_k}} [\Delta_k^{V,T}], \quad \text{where} \quad \Delta_k^{V,T} := \mathcal{L}_{\text{MLM}}(V, T; \theta_k) - \mathcal{L}_{\text{MLM}}(V, T; \theta_{k+1})$$

where $(V, T) \sim \pi_{\phi_k}(\cdot | \hat{\mathbf{S}})$ denotes a mini-batch constructed using the current scheduler π_{ϕ_k} given similarity matrix $\hat{\mathbf{S}}$. To optimize this objective, we use log-derivative trick [24] and update as:

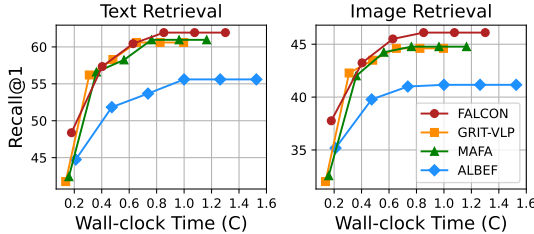
$$\phi_{k+1} = \phi_k + \gamma \cdot \mathbb{E}_{\pi_{\phi_k}} [\Delta_k^{V,T} \cdot \nabla_{\phi_k} \log \pi_{\phi_k}(V, T | \hat{\mathbf{S}})].$$

where γ denotes the step size. By leveraging the progressively optimized scheduler π_{ϕ_k} , the VLP model is guided to learn a unified semantic representation space that robustly aligns visual and textual modalities, incorporating appropriately challenging negative samples. We summarize the training loop of FALCON in Appendix C.1.

³For models in the BLIP family, the improvement can alternatively be measured using their generative objectives, such as the language modeling (LM) loss [5] or the image-text generation (ITG) loss [6].

Table 1: Performance Comparison of FALCON with existing heuristic negative mining methods on ITRT, VQA and NLVR2. All models are pretrained on the MSCOCO dataset [25].

Method	MSCOCO						NLVR2		VQA	
	Text Retrieval			Image Retrieval			dev	test-P	test-dev	test-std
	R@1	R@5	R@10	R@1	R@5	R@10				
ALBEF [4]	55.60	81.92	90.10	41.16	70.63	80.81	72.98	73.61	70.46	70.72
GRIT-VLP [8]	60.60	83.52	89.14	44.61	69.54	77.67	74.63	75.26	71.04	71.22
DiHT [11]	54.72	78.64	84.00	40.53	65.20	74.22	73.08	74.12	70.74	71.07
SRCL [10]	54.52	79.24	85.42	41.25	66.36	75.04	73.27	74.28	70.77	71.01
MAFA [9]	60.96	83.24	89.62	44.77	69.49	77.96	75.16	75.13	71.13	71.22
$q = 0.0$	18.92	55.30	72.90	20.18	58.07	74.73	72.32	73.42	69.97	70.30
$q = 0.5$	58.80	84.16	91.28	44.73	73.43	83.26	73.98	74.41	71.00	71.31
Progressive-Hardening	58.30	84.54	90.94	44.21	73.39	82.97	73.42	74.24	70.95	71.15
Progressive-Softening	59.08	84.76	91.74	44.24	73.59	82.74	73.58	74.80	70.93	71.17
FALCON	62.28	86.18	92.30	46.18	74.65	83.58	75.17	75.47	71.24	71.36



Method	Time for convergence
ALBEF	1.0C
GRIT-VLP	0.65C
MAFA	0.76C
FALCON	0.83C

Figure 6: Comparison of FALCON and baselines against relative wall clock time in Recall@1 of ITRT task. 1C represents the time it takes for ALBEF to converge.

4 Experiments

We begin by evaluating the effectiveness of FALCON in comparison to heuristic negative mining approaches in Section 4.1. Then we assess the compatibility of FALCON with the BLIP family in Section 4.2. Finally, we present additional analyses and ablation studies to further support our method in Section 4.3. Additional studies are provided in Appendix D.

Experimental Setup Unless otherwise specified, all experiments follow the training protocols established in [4, 8, 9]. The evaluation setup is described in Appendix C.6. To compute the ITC loss, we employed computationally efficient soft pseudo targets [8, 9] instead of the pseudo targets generated by a momentum model [4] for computational efficiency. For the ITM loss, the negative sample with the highest similarity to the anchor within each mini-batch is selected as the negative [8, 9]. For the ITRT task [1], evaluation was performed on the MSCOCO 5K test set. Model training was primarily conducted on a machine equipped with four NVIDIA RTX 4090 GPUs. Further experimental details are provided in Appendix C.

4.1 Comparison to Heuristic Negative Mining Methods

Comparison across downstream tasks To compare FALCON with existing heuristic negative mining methods, we pretrained all models on the MSCOCO dataset [25] and evaluated them on three downstream tasks (ITRT [1], VQA [2], NLVR [3]). As MSCOCO is a human-curated dataset with minimal annotation noise compared to web-crawled datasets [26, 27], it allows for a more isolated assessment of the effectiveness of negative sampling strategies, minimizing confounding effects from noisy image-text alignments. In addition to standard baselines used in prior work, we introduce four heuristic scheduling strategies for comparative analysis. $q = 0.0$ and $q = 0.5$ represent fixed-hardness negative sampling heuristics, where negatives are selected at constant hardness levels. Note GRIT-VLP corresponds to the $q = 1.0$ setting. Beyond these, we define two dynamic scheduling baselines: Progressive-Hardening, which gradually increases the sampled hardness level over training epochs, and Progressive-Softening, which decreases it. These schedules simulate curriculum-like strategies for hardness adjustment.

Table 2: Performance comparison on the Conceptual Captions dataset [26], both with (left) and without (right) refinement using the BLIP captioner, in addition to the MSCOCO dataset.

Method	Clean (1.1M pretrain dataset)						Noisy (1.1M pretrain dataset)					
	Text Retrieval			Image Retrieval			Text Retrieval			Image Retrieval		
	R@1	R@5	R@10	R@1	R@5	R@10	R@1	R@5	R@10	R@1	R@5	R@10
ALBEF	66.38	88.52	93.98	50.77	77.59	86.00	63.92	87.48	93.20	48.53	75.96	84.99
GRIT-VLP	66.42	86.62	91.90	48.90	73.21	80.60	67.92	88.66	93.26	50.00	75.30	82.65
MAFA	66.36	88.60	92.90	50.70	74.83	83.66	65.94	85.58	90.52	49.39	72.42	79.33
FALCON	67.34	89.06	94.26	51.81	78.78	86.67	66.00	87.90	93.98	50.47	77.52	86.02

Table 1 demonstrates that FALCON achieves significantly better performance compared to heuristic negative mining methods. Notably, hard negative sampling approaches that do not explicitly address the issue of false negatives [11, 8] suffer from degraded performance, as false negatives introduce conflicting supervision signals. Meanwhile, methods that attempt to mitigate false negatives by leveraging pretrained models [10, 9] also face inherent limitations. We believe that these approaches, which rely on fixed similarity thresholds or static filters derived from pretrained representations, are insufficient to capture the dynamic nature of optimal similarity throughout training. In contrast, FALCON adaptively adjusts its sampling strategy to reflect the temporally evolving optimal similarity range, enabling more effective hard negative selection. As a result, it consistently outperforms baseline methods across all stages of vision-language pretraining (visualized in Appendix D.2).

Comparison on relative wall clock time Figure 6 presents the performance of FALCON and baselines against relative wall clock time, where 1C denotes the total time required for ALBEF to converge. ALBEF incurs the highest per-epoch training time due to its reliance on a momentum model for generating soft labels, whereas the other methods utilize computationally efficient soft pseudo targets. Although FALCON is architecturally optimized to minimize computational overhead, it requires additional forward passes and updates for the scheduler network, leading to a moderately higher per-epoch cost compared to MAFA and GRIT-VLP. Nevertheless, FALCON achieves better performance relative to wall clock time, highlighting the effectiveness and importance of dynamically balancing the trade-off between hard and false negatives during vision-language pretraining.

Comparison on BLIP-Captioned and Noisy Datasets To further evaluate the robustness of FALCON in mitigating false negatives, we conducted experiments on web-crawled image-text pairs from the Conceptual Captions dataset [26], with and without refinement using the BLIP captioner [5], in addition to the MSCOCO dataset. This evaluation assess whether FALCON can leverage high-quality captions generated by BLIP to improve performance on noisy, web-crawled data. As shown in Table 2 (left), FALCON significantly outperforms heuristic baselines and demonstrates further performance gains as dataset size increases, compared to the results in Table 1. However, when the same web-crawled data is used without BLIP-based refinement, the performance gains become less pronounced, particularly in the text retrieval task (Table 2 (right)). We attribute this to significant noise and semantic misalignment in the original captions, which can hinder accurate estimation of the tradeoff between hard and false negatives, thereby making the learning process more complex.

4.2 Compatibility with BLIP-2

To evaluate the general applicability of FALCON to other VLP frameworks, we examined its compatibility with BLIP-2 [6], a recent VLP model demonstrating strong performance across various multimodal tasks. Unlike ALBEF, BLIP-2 replaces the masked language modeling (MLM) loss with image-grounded text generation (ITG) loss as its generative objective. Accordingly, we adopted the ITG loss as a proxy for cross-modal alignment when applying FALCON to BLIP-2. We pretrained all models on the MSCOCO dataset. As shown in Table 3, FALCON yields significant performance gains within the BLIP-2 architecture, demonstrating its applicability to BLIP-family model.

4.3 Ablation Studies

Table 4 (top) illustrates the impact of search space size on the performance of FALCON. It can be seen that increasing the search space size initially leads to performance improvements, as it enables the scheduler to more accurately select negative samples at the target hardness level specified by

Table 3: Performance Comparison of FALCON with baselines under the BLIP-2 framework.

Method	Text Retrieval			Image Retrieval			Flickr R@1	
	R@1	R@5	R@10	R1	R@5	R@10	TR	IR
BLIP-2	75.22	93.00	96.50	57.98	82.08	88.78	90.10	77.48
BLIP-2 + GRIT	73.90	93.10	96.52	57.47	80.50	87.56	90.40	77.28
BLIP-2 + MAFA	74.21	93.00	96.61	57.94	81.12	88.44	90.30	77.32
BLIP-2 + FALCON	75.56	93.50	96.90	58.52	82.39	88.98	90.90	77.72

Table 4: Ablation study analyzing the impact of search space size, training objectives, and instance-based scheduling in FALCON on IRTR performance.

Component	Setting	Text Retrieval			Image Retrieval		
		R@1	R@5	R@10	R@1	R@5	R@10
Search Space	480	58.48	84.70	91.54	44.75	73.79	82.99
	5664	61.72	86.28	92.78	46.19	74.56	83.94
	28320	61.94	85.94	92.58	46.10	74.61	83.96
Objective	$\mathcal{L}_{ITC} + \mathcal{L}_{ITM}$	57.64	84.24	91.32	43.62	73.11	82.86
	$\mathcal{L}_{ITC} + \mathcal{L}_{ITM} + \mathcal{L}_{MLM}$	57.80	84.36	91.58	44.29	73.15	82.88
	\mathcal{L}_{MLM}	61.72	86.28	92.78	46.19	74.56	83.94
Instance-based	False	58.78	84.08	90.72	44.47	73.10	82.52
	True	61.72	86.28	92.78	46.19	74.56	83.94

its action (i.e., the predicted hardness quantile). However, beyond a certain search space size, the performances are comparable to each other. This finding suggests that FALCON is robust to large search space sizes and varying distributions of hard and false negatives, as it effectively manages the trade-off between them throughout VLP. In contrast, baseline methods show performance degradation with larger search spaces, primarily due to an increased risk of false negatives (see Appendix D.3).

Table 4 (middle) presents an ablation study on the training objectives used in FALCON as proxies for cross-modal alignment improvement. The results indicate that incorporating contrastive objectives (\mathcal{L}_{ITC} and \mathcal{L}_{ITM}) degrades VLP performance, likely due to their tendency to exploit trivial (i.e., easy) negatives. In contrast, \mathcal{L}_{MLM} proves to be a more effective proxy, as it remains robust to the hardness of negatives in the current mini-batch.

Table 4 (bottom) evaluates the impact of enabling the scheduler to dynamically assign similarity level for each anchor instance. In the *instance-based false* setting, the scheduler π_ϕ selects a single similarity level shared across all anchors to construct a mini-batch used for vision-language pretraining. In contrast, the *instance-based true* setting assigns a distinct similarity level to each anchor instance to form the mini-batch. The resulting performance gap highlights the importance of instance-specific similarity selection, demonstrating that the optimal similarity level is anchor-dependent and should be adaptively determined during vision-language pretraining.

5 Conclusion

In this paper, we addressed a fundamental challenge in VLP: balancing the trade-off between informative hard negatives and misleading false negatives. We propose FALCON, a learning-based mini-batch construction strategy that dynamically schedules negative sampling to optimize this trade-off. Unlike prior heuristic approaches, FALCON explicitly learns to dynamically determine the appropriate hardness level of negatives for each anchor during mini-batch construction, improving representation quality without incurring substantial computational cost. Experimental results demonstrate that FALCON significantly outperforms heuristic negative mining strategies when integrated into both ALBEF and BLIP-based models, validating its effectiveness and generalizability across frameworks.

Limitations and future work As discussed in Section 4.1, the performance improvement of FALCON is less pronounced when applied to noisy image-text pairs. This limitation likely stems from the high level of noise and semantic misalignment in the original captions, which complicates the estimation of the trade-off between hard and false negatives and increases the overall complexity of the learning process. Developing strategies to mitigate the impact of such noisy captions (e.g., BLIP caption refining) remains an important direction for future research.

References

- [1] Andrea Frome, Greg S Corrado, Jon Shlens, Samy Bengio, Jeff Dean, Marc’ Aurelio Ranzato, and Tomas Mikolov. Devise: A deep visual-semantic embedding model. *Advances in neural information processing systems*, 26, 2013.
- [2] Stanislaw Antol, Aishwarya Agrawal, Jiasen Lu, Margaret Mitchell, Dhruv Batra, C Lawrence Zitnick, and Devi Parikh. Vqa: Visual question answering. In *Proceedings of the IEEE international conference on computer vision*, pages 2425–2433, 2015.
- [3] Alane Suhr, Stephanie Zhou, Ally Zhang, Iris Zhang, Huajun Bai, and Yoav Artzi. A corpus for reasoning about natural language grounded in photographs. *arXiv preprint arXiv:1811.00491*, 2018.
- [4] Junnan Li, Ramprasaath Selvaraju, Akhilesh Gotmare, Shafiq Joty, Caiming Xiong, and Steven Chu Hong Hoi. Align before fuse: Vision and language representation learning with momentum distillation. *Advances in neural information processing systems*, 34:9694–9705, 2021.
- [5] Junnan Li, Dongxu Li, Caiming Xiong, and Steven Hoi. Blip: Bootstrapping language-image pre-training for unified vision-language understanding and generation. In *International conference on machine learning*, pages 12888–12900. PMLR, 2022.
- [6] Junnan Li, Dongxu Li, Silvio Savarese, and Steven Hoi. Blip-2: Bootstrapping language-image pre-training with frozen image encoders and large language models. In *International conference on machine learning*, pages 19730–19742. PMLR, 2023.
- [7] Florian Schroff, Dmitry Kalenichenko, and James Philbin. Facenet: A unified embedding for face recognition and clustering. In *Proceedings of the IEEE conference on computer vision and pattern recognition*, pages 815–823, 2015.
- [8] Jaeseok Byun, Taebaek Hwang, Jianlong Fu, and Taesup Moon. Grit-vlp: Grouped mini-batch sampling for efficient vision and language pre-training. In *European Conference on Computer Vision*, pages 395–412. Springer, 2022.
- [9] Jaeseok Byun, Dohoon Kim, and Taesup Moon. Mafa: Managing false negatives for vision-language pre-training. In *Proceedings of the IEEE/CVF Conference on Computer Vision and Pattern Recognition*, pages 27314–27324, 2024.
- [10] Chaoya Jiang, Wei Ye, Haiyang Xu, Shikun Zhang, Jie Zhang, Fei Huang, et al. Vision language pre-training by contrastive learning with cross-modal similarity regulation. *arXiv preprint arXiv:2305.04474*, 2023.
- [11] Filip Radenovic, Abhimanyu Dubey, Abhishek Kadian, Todor Mihaylov, Simon Vandenhende, Yash Patel, Yi Wen, Vignesh Ramanathan, and Dhruv Mahajan. Filtering, distillation, and hard negatives for vision-language pre-training. In *Proceedings of the IEEE/CVF conference on computer vision and pattern recognition*, pages 6967–6977, 2023.
- [12] Adrian Bulat, Yassine Ouali, and Georgios Tzimiropoulos. Fff: Fixing flawed foundations in contrastive pre-training results in very strong vision-language models. In *Proceedings of the IEEE/CVF Conference on Computer Vision and Pattern Recognition*, pages 14172–14182, 2024.
- [13] Shubham Parashar, Zhiqiu Lin, Tian Liu, Xiangjue Dong, Yanan Li, Deva Ramanan, James Caverlee, and Shu Kong. The neglected tails in vision-language models. In *Proceedings of the IEEE/CVF Conference on Computer Vision and Pattern Recognition*, pages 12988–12997, 2024.
- [14] Jack Urbanek, Florian Bordes, Pietro Astolfi, Mary Williamson, Vasu Sharma, and Adriana Romero-Soriano. A picture is worth more than 77 text tokens: Evaluating clip-style models on dense captions. In *Proceedings of the IEEE/CVF Conference on Computer Vision and Pattern Recognition*, pages 26700–26709, 2024.

- [15] Jiayu Wang, Yifei Ming, Zhenmei Shi, Vibhav Vineet, Xin Wang, Sharon Li, and Neel Joshi. Is a picture worth a thousand words? delving into spatial reasoning for vision language models. *Advances in Neural Information Processing Systems*, 37:75392–75421, 2024.
- [16] Liliane Momeni, Mathilde Caron, Arsha Nagrani, Andrew Zisserman, and Cordelia Schmid. Verbs in action: Improving verb understanding in video-language models. In *Proceedings of the IEEE/CVF International Conference on Computer Vision*, pages 15579–15591, 2023.
- [17] Mike Wu, Milan Mosse, Chengxu Zhuang, Daniel Yamins, and Noah Goodman. Conditional negative sampling for contrastive learning of visual representations. *arXiv preprint arXiv:2010.02037*, 2020.
- [18] Joshua Robinson, Ching-Yao Chuang, Suvrit Sra, and Stefanie Jegelka. Contrastive learning with hard negative samples. *arXiv preprint arXiv:2010.04592*, 2020.
- [19] Kaiming He, Haoqi Fan, Yuxin Wu, Saining Xie, and Ross Girshick. Momentum contrast for unsupervised visual representation learning. In *Proceedings of the IEEE/CVF conference on computer vision and pattern recognition*, pages 9729–9738, 2020.
- [20] Manzil Zaheer, Satwik Kottur, Siamak Ravanbakhsh, Barnabas Poczos, Russ R Salakhutdinov, and Alexander J Smola. Deep sets. *Advances in neural information processing systems*, 30, 2017.
- [21] Juho Lee, Yoonho Lee, Jungtaek Kim, Adam Kosiorek, Seungjin Choi, and Yee Whye Teh. Set transformer: A framework for attention-based permutation-invariant neural networks. In *International conference on machine learning*, pages 3744–3753. PMLR, 2019.
- [22] Andrew Jaegle, Sebastian Borgeaud, Jean-Baptiste Alayrac, Carl Doersch, Catalin Ionescu, David Ding, Skanda Koppula, Daniel Zoran, Andrew Brock, Evan Shelhamer, et al. Perceiver io: A general architecture for structured inputs & outputs. *arXiv preprint arXiv:2107.14795*, 2021.
- [23] Masanari Kimura, Ryotaro Shimizu, Yuki Hirakawa, Ryosuke Goto, and Yuki Saito. On permutation-invariant neural networks. *arXiv preprint arXiv:2403.17410*, 2024.
- [24] Richard S Sutton, David McAllester, Satinder Singh, and Yishay Mansour. Policy gradient methods for reinforcement learning with function approximation. *Advances in neural information processing systems*, 12, 1999.
- [25] Tsung-Yi Lin, Michael Maire, Serge Belongie, James Hays, Pietro Perona, Deva Ramanan, Piotr Dollár, and C Lawrence Zitnick. Microsoft coco: Common objects in context. In *Computer vision—ECCV 2014: 13th European conference, zurich, Switzerland, September 6-12, 2014, proceedings, part v 13*, pages 740–755. Springer, 2014.
- [26] Piyush Sharma, Nan Ding, Sebastian Goodman, and Radu Soricut. Conceptual captions: A cleaned, hypernymed, image alt-text dataset for automatic image captioning. In *Proceedings of the 56th Annual Meeting of the Association for Computational Linguistics (Volume 1: Long Papers)*, pages 2556–2565, 2018.
- [27] Vicente Ordonez, Girish Kulkarni, and Tamara Berg. Im2text: Describing images using 1 million captioned photographs. *Advances in neural information processing systems*, 24, 2011.
- [28] Jinyu Yang, Jiali Duan, Son Tran, Yi Xu, Sampath Chanda, Liqun Chen, Belinda Zeng, Trishul Chilimbi, and Junzhou Huang. Vision-language pre-training with triple contrastive learning. In *Proceedings of the IEEE/CVF Conference on Computer Vision and Pattern Recognition*, pages 15671–15680, 2022.
- [29] Yan Zeng, Xinsong Zhang, and Hang Li. Multi-grained vision language pre-training: Aligning texts with visual concepts. *arXiv preprint arXiv:2111.08276*, 2021.
- [30] Junyu Bi, Daixuan Cheng, Ping Yao, Bochen Pang, Yuefeng Zhan, Chuanguang Yang, Yujing Wang, Hao Sun, Weiwei Deng, and Qi Zhang. VI-match: Enhancing vision-language pretraining with token-level and instance-level matching. In *Proceedings of the IEEE/CVF International Conference on Computer Vision*, pages 2584–2593, 2023.
- [31] Yiren Jian, Chongyang Gao, and Soroush Vosoughi. Bootstrapping vision-language learning with decoupled language pre-training. *Advances in Neural Information Processing Systems*, 36:57–72, 2023.

- [32] Chaoya Jiang, Haiyang Xu, Wei Ye, Qinghao Ye, Chenliang Li, Ming Yan, Bin Bi, Shikun Zhang, Fei Huang, and Songfang Huang. Bus: Efficient and effective vision-language pre-training with bottom-up patch summarization. In *Proceedings of the IEEE/CVF International Conference on Computer Vision*, pages 2900–2910, 2023.
- [33] Ching-Yao Chuang, Joshua Robinson, Yen-Chen Lin, Antonio Torralba, and Stefanie Jegelka. Debaised contrastive learning. *Advances in neural information processing systems*, 33:8765–8775, 2020.
- [34] Tsai-Shien Chen, Wei-Chih Hung, Hung-Yu Tseng, Shao-Yi Chien, and Ming-Hsuan Yang. Incremental false negative detection for contrastive learning. *arXiv preprint arXiv:2106.03719*, 2021.
- [35] Tri Huynh, Simon Kornblith, Matthew R Walter, Michael Maire, and Maryam Khademi. Boosting contrastive self-supervised learning with false negative cancellation. In *Proceedings of the IEEE/CVF winter conference on applications of computer vision*, pages 2785–2795, 2022.
- [36] Tianlong Chen, Xiaohan Chen, Wuyang Chen, Howard Heaton, Jialin Liu, Zhangyang Wang, and Wotao Yin. Learning to optimize: A primer and a benchmark. *Journal of Machine Learning Research*, 23(189):1–59, 2022.
- [37] Junjie Yang, Xuxi Chen, Tianlong Chen, Zhangyang Wang, and Yingbin Liang. M-12o: Towards generalizable learning-to-optimize by test-time fast self-adaptation. *arXiv preprint arXiv:2303.00039*, 2023.
- [38] Wenqing Zheng, Tianlong Chen, Ting-Kuei Hu, and Zhangyang Wang. Symbolic learning to optimize: Towards interpretability and scalability. *arXiv preprint arXiv:2203.06578*, 2022.
- [39] Marcin Andrychowicz, Misha Denil, Sergio Gomez, Matthew W Hoffman, David Pfau, Tom Schaul, Brendan Shillingford, and Nando De Freitas. Learning to learn by gradient descent by gradient descent. *Advances in neural information processing systems*, 29, 2016.
- [40] Olga Wichrowska, Niru Maheswaranathan, Matthew W Hoffman, Sergio Gomez Colmenarejo, Misha Denil, Nando Freitas, and Jascha Sohl-Dickstein. Learned optimizers that scale and generalize. In *International conference on machine learning*, pages 3751–3760. PMLR, 2017.
- [41] Irwan Bello, Barret Zoph, Vijay Vasudevan, and Quoc V Le. Neural optimizer search with reinforcement learning. In *International Conference on Machine Learning*, pages 459–468. PMLR, 2017.
- [42] Ke Li and Jitendra Malik. Learning to optimize neural nets. *arXiv preprint arXiv:1703.00441*, 2017.
- [43] Myunsoo Kim, Donghyeon Ki, Seong-Woong Shim, and Byung-Jun Lee. Adaptive non-uniform timestep sampling for diffusion model training. *arXiv preprint arXiv:2411.09998*, 2024.
- [44] Bryan A Plummer, Liwei Wang, Chris M Cervantes, Juan C Caicedo, Julia Hockenmaier, and Svetlana Lazebnik. Flickr30k entities: Collecting region-to-phrase correspondences for richer image-to-sentence models. In *Proceedings of the IEEE international conference on computer vision*, pages 2641–2649, 2015.
- [45] Ranjay Krishna, Yuke Zhu, Oliver Groth, Justin Johnson, Kenji Hata, Joshua Kravitz, Stephanie Chen, Yannis Kalantidis, Li-Jia Li, David A Shamma, et al. Visual genome: Connecting language and vision using crowdsourced dense image annotations. *International journal of computer vision*, 123:32–73, 2017.

A Related Works

Vision-language pre-training (VLP) The training paradigm introduced by ALBEF [4], which jointly optimizes the ITC, ITM, and MLM objectives, has served as the foundation for many subsequent VLP frameworks [5, 6, 28, 29, 30, 31, 32, 8, 9]. Given the high sensitivity of both ITC and ITM objectives to the difficulty of negative samples, several studies have proposed strategies to enhance vision-language pretraining by leveraging hard negative sampling. For example, ALBEF [4] computed the ITM loss by sampling in-batch hard negatives based on contrastive similarity scores computed within the current mini-batch. DiHT [11] proposed an importance sampling approach to upweight harder negatives based on their similarity to the anchor. GRIT-VLP [8] enhances hard negative sampling by introducing the Grouped Mini-batch Sampling (GRIT) strategy, which constructs mini-batches composed of the most semantically similar image-text pairs retrieved from a large candidate pool M . This increases the chance of including informative hard negatives within each batch for both ITC and ITM losses.

False negatives in VLP While several prior works have proposed strategies to mitigate the impact of false negatives in the vision domain [18, 33, 34, 35, 17], the increased risk of false negatives introduced by hard negative sampling remains relatively underexplored in the context of vision-language pretraining. [10] proposed Similarity-Regulated Contrastive Learning (SRCL), which adjusts the contrastive loss by weighting negative samples according to their cross-modal similarity to the anchor, where the similarity is initially estimated using a pretrained model and progressively refined during training. By assigning lower weights to semantically similar negatives, SRCL mitigates the over-penalization of false negatives during contrastive learning. More recently, [9, 12] demonstrated that converting false negatives into positives using a strong pretrained model can improve the performance on downstream tasks. These findings highlight a fundamental trade-off between hard and false negatives, emphasizing its significant impact on the learned representations. However, such methods rely heavily on pretrained models and fixed heuristic thresholds (e.g., ITM score cutoffs) to identify false negatives, which may limit their robustness and generalizability across diverse datasets and training conditions. In contrast, we propose a learning-based approach that adaptively balances the trade-off between hard and false negatives throughout the training process, without relying on fixed heuristics or external pretrained models.

Learning to optimize (L2O) L2O is a research paradigm in machine learning that aims to automatically learn optimization algorithms from data, rather than relying on handcrafted update rules. Early works in L2O typically adopted a meta-learning framework, where an optimizer is parameterized (e.g., via neural networks) and trained across a collection of optimization tasks [36, 37, 38]. In this framework, a meta-training set composed of multiple task-specific training and validation dataset pairs is used to guide the optimizer to generalize across tasks. Based on the meta-training set, L2O methods learn parameter update rules that minimize validation loss, either through supervised learning [39, 40] or reinforcement learning [41, 42]. Recent advances have begun to challenge these assumptions by introducing optimization policies that must learn and adapt in the absence of a predefined meta-training set [43]. In this paper, we propose an online optimization approach that constructs mini-batches to balance the tradeoff between hard and false negatives, without relying on any meta-training dataset.

B Proof of Proposition 1

Proposition 1. *Let $\mathcal{V} = \{v_1, \dots, v_{|\mathcal{V}|}\}$ denote the set of images and $\mathcal{T} = \{t_1, \dots, t_{|\mathcal{T}|}\}$ the set of texts. Define $\mathcal{R} \subseteq \mathcal{V} \times \mathcal{T}$ as the binary relation of semantic compatibility within the Cartesian product of image and text set, where $(v, t) \in \mathcal{R}$ implies that t is a valid description of v . Let $\mathcal{P} \subset \mathcal{R}$ denote the set of ground-truth positive pairs available to the learner, such that any pair $(v, t) \notin \mathcal{P}$ is treated as negative during vision-language pretraining (VLP). Then, the probability of sampling a false negative remains **strictly positive** unless $\mathcal{P} = \mathcal{R}$, an assumption that is infeasible in practice.*

Proof. Define

$$\rho = \frac{|\mathcal{R}|}{|\mathcal{V}||\mathcal{T}|} \quad (\text{valid match density}), \quad \kappa = \frac{|\mathcal{P}|}{|\mathcal{R}|} \quad (\text{ground-truth label coverage}). \quad (2)$$

When a uniform negative sampler draws an image-text pair from $(\mathcal{V} \times \mathcal{T}) \setminus \mathcal{P}$,

$$\Pr[\text{false neg.}] = \frac{|\mathcal{R}| - |\mathcal{P}|}{|\mathcal{V}||\mathcal{T}| - |\mathcal{P}|} = \frac{(1 - \kappa)\rho}{1 - \kappa\rho} \geq (1 - \kappa)\rho. \quad (3)$$

Since $\rho > 0$ for any image-caption dataset and $\kappa < 1$ by many-to-many correspondence nature between two modalities, the probability of sampling a false negative is strictly positive. \square

C Experimental Details

C.1 Algorithms

This section presents the pseudo-code for mini-batch construction and the overall training loop of FALCON. Algorithm 1 outlines the procedure for constructing a mini-batch index set \mathcal{I} . The process begins by sampling an initial anchor from the pool of unselected index set \mathcal{U} , followed by selecting the remaining $B - 1$ indices based on quantile values q drawn from the scheduler policy π_ϕ . Algorithm 2 describes the overall vision-language pretraining loop with a search space of size $|M|$. The image-text similarity matrix \mathbf{S} is computed from the [CLS] embeddings in the current queue. Subsequently, a mini-batch is constructed using Algorithm 1. The vision-language model parameters θ are then updated via gradient descent, while the scheduler parameters ϕ are updated through gradient ascent.

Algorithm 1 Compose Mini-batch Index Set

Input: Similarity matrix \mathbf{S} , unselected index set \mathcal{U} , batch size B , scheduler π_ϕ

```

1: Initialize mini-batch index set  $\mathcal{I} = \{\}$ 
2: Select quantiles and normalize  $\mathbf{S}$  to get  $\hat{\mathbf{S}}$ 
3:  $q \sim \pi_\phi(\cdot | \hat{\mathbf{S}})$ 
4:  $i = \text{Uniform}(\mathcal{U})$ 
5:  $\mathcal{I} \leftarrow \mathcal{I} \cup \{i\}$ 
6:  $\mathcal{U} \leftarrow \mathcal{U} \setminus \{i\}$ 
7: for  $B - 1$  do
8:    $i \leftarrow \text{index of } q\text{-quantile of } \{\mathbf{S}_{i,j} \mid j \in \mathcal{U}\}$ 
9:    $\mathcal{I} \leftarrow \mathcal{I} \cup \{i\}$ 
10:   $\mathcal{U} \leftarrow \mathcal{U} \setminus \{i\}$ 
11: end for
12: return  $\mathcal{I}$ 
```

Algorithm 2 VLP with Mini-batch Scheduler (for i -th search space M)

Input: VLP parameter θ , scheduler parameter ϕ , Vision dataset \mathcal{V} , Text dataset \mathcal{T} , learning rate η, γ

```

1: Compute pairwise similarity matrix  $\mathbf{S}$  between  $\mathcal{V}, \mathcal{T}$  in search space  $M$ 
2: Initialize unselected index set  $\mathcal{U} = \{0, \dots, |M| - 1\}$ 
3: for gradient step  $k \in \{0, 1, \dots, \lfloor |M|/B \rfloor - 1\}$  do
4:   Get mini-batch index  $\mathcal{I}$  with Algorithm 1
5:   Construct mini-batch  $V, T$  as samples at indices  $\mathcal{I} + i \cdot |M|$  from  $\mathcal{V}, \mathcal{T}$ 
6:    $\theta_{k+1} = \theta_k - \eta \cdot \nabla_{\theta_k} \mathcal{L}_{\text{VLP}}(V, T; \theta_k)$ 
7:    $\Delta_k = \mathcal{L}_{\text{MLM}}(\theta_k) - \mathcal{L}_{\text{MLM}}(\theta_{k+1})$ 
8:    $\phi_{k+1} = \phi_k + \gamma \cdot \Delta_k \nabla_{\phi_k} \log \pi_{\phi_k}(q | \hat{\mathbf{S}})$ 
9: end for
```

C.2 Implementation Details of the Mini-batch Construction Process

At the beginning of vision-language pretraining, the queue does not yet contain a sufficient number of cached [CLS] embeddings to construct the similarity matrix \mathbf{S} . Accordingly, we follow GRIT-VLP [8, 9] and adopt a standard uniform mini-batch sampling procedure during the first epoch, without training or applying the scheduler π_ϕ . From the second epoch onward, cached image and text embeddings from the previous epoch are used to compute similarity matrices, enabling the scheduler to guide mini-batch construction. This design introduces a natural warm-start effect, providing a stable and efficient initialization for the learning-based mini-batch sampling scheduler π_ϕ . As training progresses, the cached embeddings are updated epoch by epoch to reflect the current state of the VLP model, enabling the scheduler to make decisions that are aligned with the evolving structure of the embedding space.

To prevent overfitting, we apply instance-level scheduling at the end of each epoch to ensure that the search space does not consist of fixed instances throughout training [8]. This shuffling improves generalization by exposing the scheduler to a more diverse and representative set of training instances over time.

C.3 Implementation Details of Baseline Methods

For ALBEF [4], GRIT-VLP [8], MAFA [9], and BLIP-2 [6], we conduct experiments using the official codebases released by the original authors. For methods without publicly available implementations (DiHT [11] and SRCL [10]), we implemented the loss functions described in the respective papers using the ALBEF codebase as a foundation.

For quantile-based heuristic baselines, we adopt the mini-batch grouping procedure of GRIT-VLP, modifying the default quantile $q = 1.0$ according to each heuristic strategy. These include fixed quantile settings, such as $q = 0.5$ and $q = 0.0$, as well as dynamic schedules in which the quantile is progressively increased (hardening) or decreased (softening) over the course of training.

C.4 Hyperparameter Settings

We use the same backbone architecture and data augmentation strategy as ALBEF. The detailed hyperparameter settings are summarized in Table 5. For all remaining configurations, we follow the settings used in GRIT-VLP.

Table 5: Hyperparameter settings used for FALCON

Category	Hyperparameter	Setting
VLP model	Image Resolution	256
	Embedding Dimension	256
	Batch Size B	96
	Masking Probability	0.5
	Search Space size $ M $	{2400, 5664, 28320}
	Pretraining Epochs	20
	Optimizer	AdamW($\beta = [0.9, 0.999]$, $\lambda = 0.02$)
	learning rate γ	scheduled
Scheduler π	m for Subsampling	100
	Hidden Layer Dimension	256
	# Residual Block	2
	Optimizer	AdamW($\beta = [0.9, 0.999]$, $\lambda = 0.01$)
	learning rate η	1e-4

C.5 Pretraining dataset size

Table 6 shows the statistics of the pretraining dataset we used. For Conceptual Captions dataset, we used the preprocessed version provided by the original authors of BLIP [5].⁴

Table 6: Statistics of the pretraining dataset

	COCO	CC (Filtered web caption)	CC (Synthetic caption by BLIP)
image	113K	567K	567K
text	567K	567K	567K

C.6 Details on Downstream tasks

For all retrieval tasks (COCO IRTR [25], Flickr IRTR [44]), we evaluate the pretrained models directly without any task-specific finetuning. For NLVR2 [3], we follow the protocol established in ALBEF [4], performing an additional pretraining stage on the COCO dataset to adapt the model for reasoning over paired images, followed by finetuning on the NLVR2 dataset for 10 epochs. For the VQA task [2], we finetune the pretrained model for 8 epochs using both the training and validation splits of the COCO and Visual Genome datasets [45], following standard practice in prior work [4, 8, 9].

⁴<https://github.com/salesforce/BLIP?tab=readme-ov-file#pre-training-datasets-download>

D Additional Experiment results

D.1 Visualization of FALCON

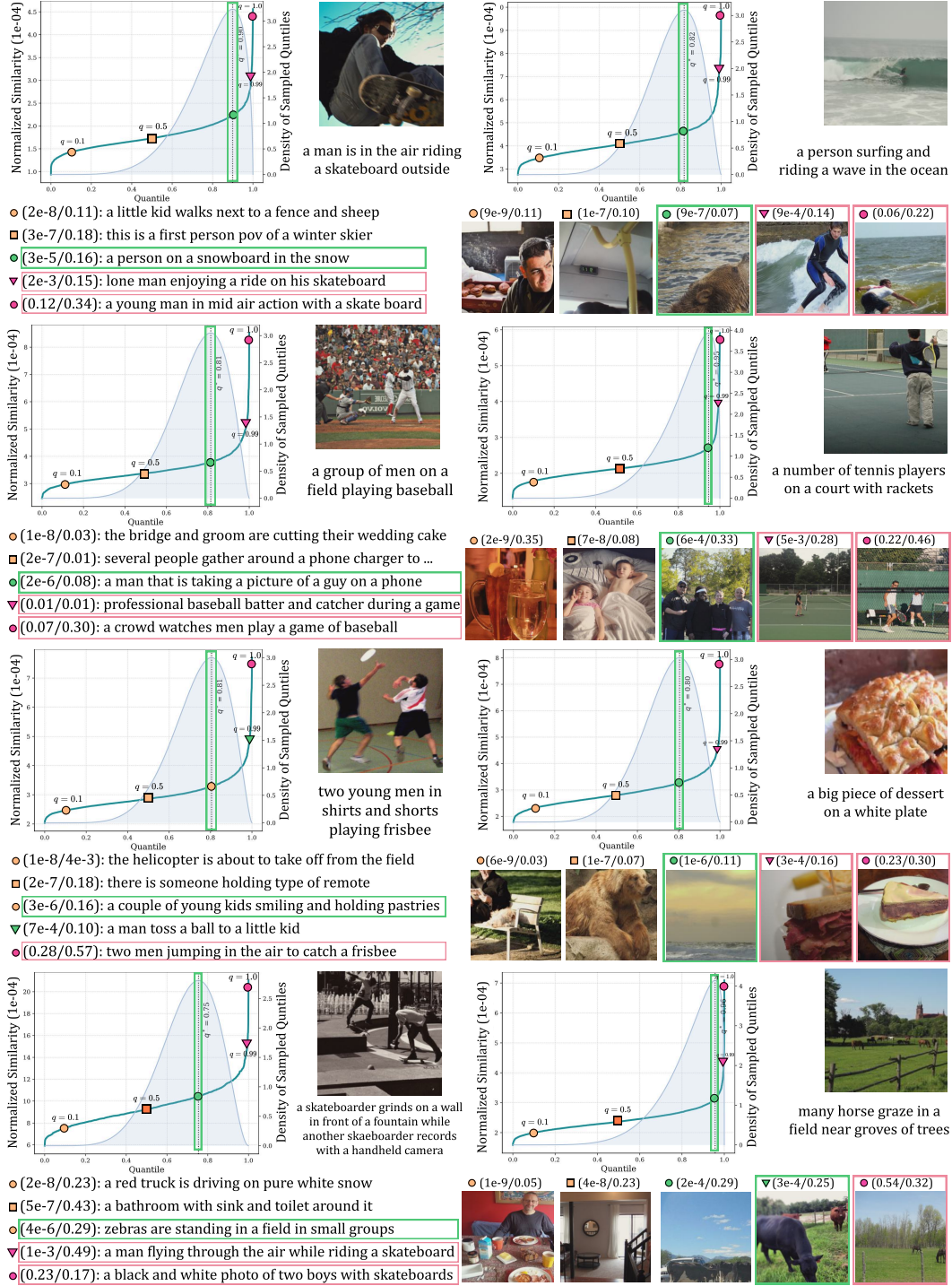


Figure 7: Additional anchor-specific negative sampling visualizations. We highlight the mode of scheduler distribution in green and genuine false negatives in red. Each negative is annotated with “(one-way similarity / ITM score)” and its hardness is color-coded as in Figure 1.

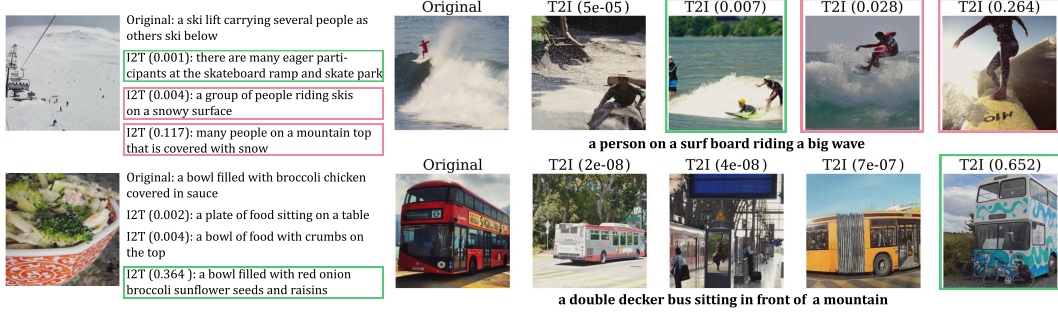


Figure 8: Image-to-Text (Left) and Text-to-Image (Right) examples of negative sampling under FALCON’s quantile-based scheduling strategy. Negative candidates are drawn from similarity score quantiles [0.8, 0.9, 1.0] for I2T and [0.5, 0.8, 0.9, 1.0] for T2I. The negative sample selected by FALCON is highlighted in green and the genuine false negative sample is highlighted in red.

D.2 Comparison with Heuristic Negative Mining Methods Across Training Epochs

We evaluate FALCON against baseline methods over the full course of training epochs on the image-text retrieval (IRTR) downstream task. All models are pretrained on the MSCOCO dataset. Throughout training, FALCON consistently outperforms all heuristic baselines across all epochs and recall metrics, highlighting its effectiveness in adaptively selecting negative samples with appropriate hardness during VLP mini-batch construction.

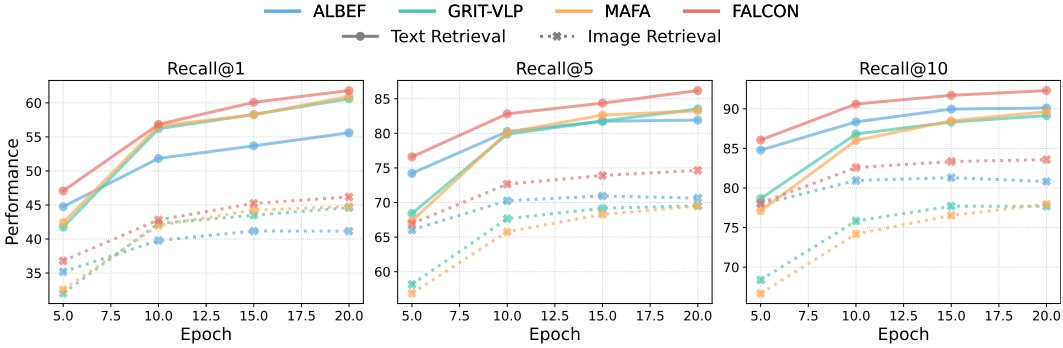


Figure 9: Performance comparison of VLP models across vision-language pretraining epochs on IRTR task. Recall@K ($K = 1, 5, 10$) is reported separately for text-to-image (solid lines) and image-to-text (dotted lines) retrieval.

D.3 Hyperparameter Sweeping in Baselines

Table 7: Retrieval performance of two baseline models (GRIT-VLP, MAFA) pretrained on the MSCOCO dataset under various hyperparameter configurations. We vary the search space size $|M|$ for both methods. For MAFA, we additionally sweep the threshold parameter τ , which determines whether a given image-text pair is classified as a false negative based on its similarity score.

Component	Setting	Text Retrieval			Image Retrieval		
		R@1	R@5	R@10	R@1	R@5	R@10
GRIT-VLP	$ M = 1920$	60.60	83.52	89.14	44.61	69.54	77.67
	$ M = 4800$	55.08	78.10	84.60	39.06	62.57	71.67
MAFA	$ M = 1920, \tau = 0.98$	60.96	83.24	89.62	44.77	69.49	77.96
	$ M = 4800, \tau = 0.98$	54.86	77.04	84.36	39.57	63.13	72.20
	$ M = 1920, \tau = 0.80$	40.62	68.04	78.20	33.10	57.75	67.63